ВЗАИМОДЕЙСТВИЕ РЕЛЯТИВИСТСКИХ ЧАСТИЦ С КРИСТАЛЛАМИ И ВЕЩЕСТВОМ

ULTRA RELATIVISTIC ELECTRON BEAM SPATIAL SIZE ESTIMATION FROM ANGULAR DISTRIBUTION OF THEIR RADIATION IN THIN CRYSTALS

Yu.A. Goponov[1], M.A. Sidnin[1], K. Sumitani[2], Y. Takabayashi[2], I.E. Vnukov[1]
[1]Belgorod National Research University, Belgorod, Russia;
[2]SAGA Light Source, 8-7 Yayoigaoka, Tosu, Saga 841-0005, Japan
E-mail: vnukov@bsu.edu.ru

The use of ultra relativistic electron (positron) emission in thin crystals to estimate particle beam spatial sizes for projected electron-positron colliders is proposed. The existing position-sensitive X-ray range detectors and the average path of secondary electrons in a detector restrict the minimum value of the measured beam size to a level of approximately 10 μm, which is far greater than the planned sizes of collider beams. We propose to estimate the electron (positron) beam divergence over the diffracted transition radiation from angular distribution measurements. The spatial size can be obtained from the calculated beam emittance or the experimental emittance, which is measured during the earlier stage of acceleration using optical methods. The problem of crystal destruction under the influence of a high intensity electron beam is discussed. The use of surface parametric X-ray radiation, where the problem of crystal destruction is almost absent, to measure the electron beam parameters is discussed.

PACS: 29.20.db, 29.27.Fh

INTRODUCTION

One of the most important parameters that determine the efficiency of projected electron-positron linear colliders [1, 2] is the luminosity:

$$L = \frac{n_b N^2 f_{rep}}{4\pi\sigma_x\sigma_y} H_D \ , \qquad (1)$$

where n_b is the number of bunches, N is the bunch population, f_{rep} is the repetition rate, H_D is the luminosity enhancement factor, and σ_x and σ_y are the characteristic beam sizes in the horizontal and vertical directions, respectively. The estimated luminosity L of the International Linear Collider (ILC) is approximately 10^{34} cm^{-2}·s^{-1} and higher, due to the small size of the beam at the interaction point of 100×5 nm^2 (σ_x×σ_y) [1]. Invasive [3] and non-invasive [4, 5] methods developed to determine the transverse beam size based on the registration of optical radiation from metal foils set in the accelerator cannot ensure measurement of the beam parameters with such small sizes, due to coherent effects in the radiation [6].

One method that can provide non-invasive measurement of the spatial dimensions of an ultra-fast electron beam is to use the Shintake monitor, based on the interaction of electrons with a target of laser interference fringes, and record the scattered Compton photons emitted in the direction of the electron beam [7]. Recently, this method has been used to measure the dimensions of the KEK-ATF beam in the range of 20 nm to several microns with an accuracy of no more than 10% [8]. To use this method, the electron beam must be bent by a magnet after interaction; therefore, its use under the conditions of the ILC would require significant additional expenditure. For the same reason it cannot be used in a collider regime where there are two simultaneous particle beams or for intermediate diagnostics and control of the beams inside the accelerator during the acceleration process.

Another way to address this issue could be a decrease of the detected radiation wavelength by switching to the X-ray frequency range and employing the mechanism of parametric X-ray radiation (PXR) proposed in Refs. [9] and [10]. In the first approximation, PXR may be considered as coherent scattering of the electromagnetic field of a particle on the electron shells of periodically arranged target atoms [11, 12]. PXR has also been referred to as the result of self-field diffraction of a fast charged particle moving through a crystal [13].

By analogy with X-ray diffraction in crystals, there are two approaches to the description of PXR. The kinematic approximation suggests that the multiple reflections of PXR photons at crystal planes are negligibly small. If this condition is not satisfied, then it is necessary to use dynamical theory. PXR can also be described as a coherent polarization bremsstrahlung of relativistic charged particles in a crystal [14] (see also [15]). As part of this approach, it has been shown [16] that for perfect crystals the contribution of dynamic effects is not more than 10%; therefore, the kinematic approximation should be sufficient to describe the experimental data.

For fast electrons, PXR is always accompanied by radiation diffracted in the crystal, which is generated directly inside the target or on its surface [17, 18]. In the first case, diffracted bremsstrahlung (DB) is considered, while in the second case, diffracted transition radiation (DTR) is considered. The former is dominant under the condition $\omega >> \gamma\omega_p$, where ω is the photon energy, γ is the Lorentz factor, and ω_p is the plasma frequency of the medium, whereas the latter is dominant under the opposite condition. If the condition $\omega \sim \gamma\omega_p$ is true, then the contributions of both radiation mechanisms are observed.

The choice of radiation mechanism corresponds with the large angles of PXR emission in the direction of the electron motion and it can be detected relatively easily

with conventional X-ray detectors. Numerous experimental works (see, for example, [19] and references therein) have demonstrated that the kinematic PXR theory describes the results of measurements for electron energies from a few mega electron-volt to several gig electron-volt with accuracy better than 10…15%.

A study on the influence of the electron beam size on the PXR spatial distribution from 855 MeV electrons in a 50 μm thick silicon crystal using a high-resolution X-ray camera (HR) [20] based on a thin scintillator coupled waveguides with a CCD matrix [21] has confirmed that estimation of the electron beam size is possible with such measurements. Electron beam size measurements for energy of 255 MeV using the PXR spatial distribution in a 20 μm thick silicon crystal made with a coordinate detector based on an imaging plate (IP) [22] coincided with that using optical transition radiation (OTR) [23].

Unlike the Shintake monitor, a device that can realize this method of electron beam size measurement can be used at any stage of acceleration, requires significantly less expenditure, and can be relatively easily integrated into the accelerator control system by replacing the existing beam monitors based on OTR [3], optical diffraction radiation (ODR) [4], and Smith-Purcell radiation [5]. The change in the ratio of PXR and diffracted real photons of TR and bremsstrahlung with an increase of electron energy up to 100…500 GeV [26] and a decrease in the size of the beam have yet to be clarified.

Thus, the unresolved problems, yet obvious advantages, of using the X-ray emission of electrons in thin crystals to diagnose the parameters of ultra-high energy electron beams suggests that research in this area is important and relevant.

RESULTS AND DISCUSSION

1. GENERAL CONSIDERATIONS

In the experiment, all the radiation mechanisms generated at the Bragg angles are implemented simultaneously. The basic formulae and approaches for each mechanism that was used for calculations are presented in Refs. [18] and [24]. The kinematic PXR theory describes the results of measurements quite well; therefore, the PXR yield was calculated by using a PXR spectral-angular distribution formula obtained in the kinematic approximation in Ref. [27]. To determine the yield of the diffracted radiation, it is necessary to determine the reflectivity of the crystal. Here we used the method described in Ref. [24], which is based on the approach proposed in Ref. [18] and allows multiple Bragg re-scattering, absorption, and scattering photons due to processes that are not associated with diffraction to be taken into account.

Using X-rays to measure the size of a fast electron beam by the PXR mechanism [10, 21, 23] is restricted to the minimum size that can be measured with coordinate detectors of X-ray range. The spatial resolution of the devices used in the experiments [10, 21, 23] was evaluated to be approximately 50 μm for photon energies up to 100 keV [20, 22]. For a fixed photon energy as an estimation of the spatial resolution of these devices, the root-mean-squared path of the secondary electrons in the detector (photoelectrons and Auger electrons) may be taken in account, providing the oxidation of Eu^{2+} to Eu^{3+} in the case of an IP and the scintillation yield in the case of an X-ray camera. The path value is dependent on the energy of the detected radiation, determined according to the crystal used and the observation angle, and the working medium of the detector. The thickness of an IP and the scintillator of an X-ray camera is less than 100 μm; therefore, the contribution of characteristic X-ray radiation photons to the formation of the detected spatial distribution in a first approximation may be ignored.

Here, we consider the use of devices such as the X-ray camera, because in the case of the IP, the angular distribution cannot be measured in real-time [11]. Consequently, such a device cannot be used for fast collection of the electron beam parameters. In contrast, the efficiency of an X-ray camera is relatively high. In the experiment [21], the spatial radiation distribution measurement for one crystal orientation took 4 seconds at an average current of 0.5 μA, which was sufficient for confident registration of the angular distribution with $\sim 10^{13}$ electrons. This value is close to the number of electrons for a single ILC spill ($\approx 2.6 \cdot 10^{13}$ electrons/cycle) [1]. Taking into account the significantly higher DTR angular density compared with that for PXR with high-energy electrons [26], the number of electrons required for reliable registration of the spatial distribution of the radiation would be several orders of magnitude smaller.

For the experimental conditions [21] (absorption of the first order reflection photons energy of 16 keV occurs on the *L*-shell of gadolinium), the energy of secondary electrons is approximately 8 keV, which corresponds to an approximately 1 μm path of the secondary electrons [27]. For other observation angles and higher reflection orders, this value may be increased to 10…30 μm. The typical size of a CCD pixel is approximately 10 μm. In particular, the pixel dimensions of the X-ray camera are 11.6×11.2 μm [20]. The dimension of the projected collider beam is approximately 5…100 nm [1, 2], which is significantly less than ten microns; therefore, direct measurement of the spatial sizes of the electron beam by transition to the X-ray range and the PXR mechanism is not feasible due to the characteristics of the existing detectors.

Therefore, we propose to measure the beam angular divergence instead of the beam size. As described in Refs. [1, 2], the beam divergence is not so small (a few tens of μrad > γ^{-1}), although the beam size is extremely small. It is known that the main parameter that characterizes the dynamics of the particle motion in an accelerator is the beam emittance $\varepsilon_{x,y} = \sigma_{x,y}\theta_{x,y}$, where $\sigma_{x,y}$ and $\theta_{x,y}$ are the respective size and divergence of the beam in the horizontal and vertical directions. Therefore, measurement of the electron beam angular distribution and divergence in one plane provides information regarding the beam size in this plane from the emittance for this direction. The required value for emittance can be obtained from measurements conducted in the early stages of acceleration using conventional methods or calculation results (see, for example, Ref. [1, 2]).

Conventional methods based on OTR and ODR cannot provide the required accuracy for measurement of

the angular distribution of a particle accelerated to the final energy due to coherent effects. The characteristic angular size of a PXR photon beam is weakly dependent on the electron energy and can be written in the form [28]:

$$\Theta_{ph} = \sqrt{\gamma^{-2} + \omega_p^2 / \omega^2 + \sigma_{ms}^2}\,, \qquad (2)$$

where σ^2_{ms} is the root-mean-squared angle of multiple scattering of particles in a crystal. For observation angles of $\Theta_D < 45^\circ$, $\Theta_{ph} \approx 2\ldots5$ mrad, depending on the photon energy and the crystal used, exceed the divergence of the electron beam at the interaction point $\theta \approx 40$ and 15 μrad in the horizontal and vertical planes, respectively, for the ILC [1], and exceed the divergence of 7 to 10 μrad for the Compact Linear Collider (CLIC) [2]. Therefore, measurements of the angular distribution of PXR photons cannot help in the estimation of the electron beam divergence incident on the crystal.

PXR is always accompanied by diffracted real photons of bremsstrahlung and TR emitted in a strictly Bragg direction. The ratio between the yields of PXR photons and diffracted real photons is determined by the crystal thickness and the experimental conditions. Recently, in Ref. [26], it was reported that the ratio between the angular density of PXR intensity and DTR one is significantly changed with an increase in the electron energy up to tens GeV and higher. The angular density of the DTR intensity becomes far higher than that for PXR.

2. CALCULATION RESULTS

Fig. 1 shows the calculation results for the vertical angular distribution of radiation with the experimental geometry [21] and the first order reflections. The detailed calculation method is described in Refs. [24] and [25]. The electron beam is incident on a 50 μm thick silicon crystal and the (220) reflection is investigated. The detection system is located at a distance of 1 m from the crystal at an angle $\Theta_D = 2\Theta_B = 22.5^\circ$. Size of the square detector is 0.05×0.05 mm, moved down through the reflex center with 0.05 mm steps. Curves 1 and 2 are the calculation results for the angular distributions of PXR and DTR for electrons energy of 1 GeV.

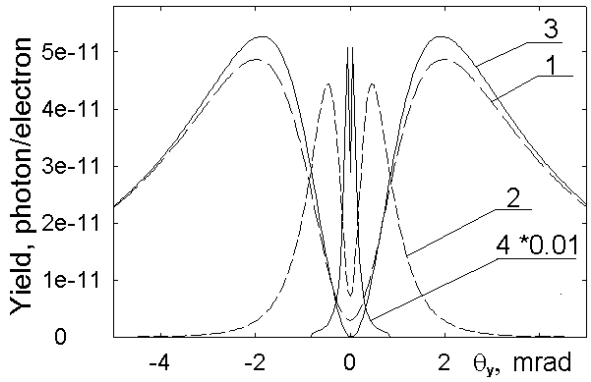

Fig. 1. Vertical distribution of the X-ray yield for the experimental geometry [21], and the first order reflection: 1 – PXR for E=1 GeV; 2 – DTR for E=1 GeV; 3 – PXR for E=10 GeV; 4 – DTR for E=10 GeV

Curves 3 and 4 are the same results for electrons energy of 10 GeV. The diffracted bremsstrahlung contribution is negligibly small and is not represented for conditions of ω = 16.55 keV<<$\gamma\omega_p \approx$60 and 600 keV for electron energies of 1 and 10 GeV, respectively.

Fig. 1 shows that the increase of the electron energy did not change the PXR angular distribution significantly. The small difference between the distributions for different energies is due to the lower multiple scattering for higher energy electrons. This difference is very large for DTR angular distributions because the TR intensity is proportional to the electron energy and the characteristic size of the TR angular cone is approximately γ^{-2}; therefore, the DTR angular distribution for higher energy electrons is much narrower.

For larger electron energy and smaller electron beam divergence compared with Θ_{ph}, the central part of the radiation reflex will be a low pedestal associated with the registration of PXR photons. The narrow bright peak width for γ^{-1} that corresponds to the contribution of DTR is located in the center of the PXR angular distribution. For ILC conditions, the electron (positron) beam divergence at the interaction point θ_e is approximately 15…20 μrad over a wide range of particle energies [1], which is significantly higher than the characteristic radiation angle $\gamma^{-1} \sim 1\ldots3$ μrad for particle energies above 200 GeV. Therefore, the shape of the radiation angular distribution is not dependent on the particle energy, but is defined only by the divergence of the electron (positron) beam.

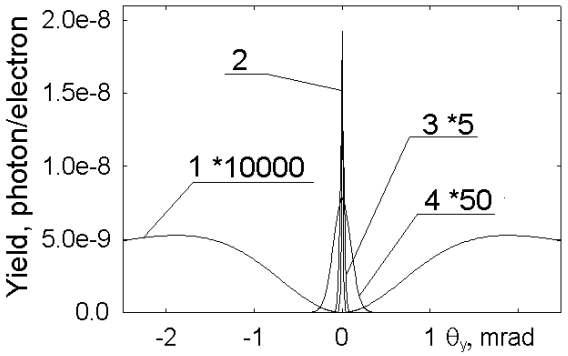

Fig. 2. Vertical distribution of the X-ray yield for an electron energy of 200 GeV and the first order reflection: 1 – PXR; 2 – DTR for $\theta_e < \gamma^{-1}$; 3 – DTR for θ_e=20 μrad; 4 – DTR for θ_e=100 μrad

To illustrate this, Fig. 2 shows the calculation results for the vertical angular distribution of the radiation for a beam of electrons with an energy of 200 GeV incident on a 50 μm thick silicon crystal, where the (220) reflection is used. The detection system is located at a distance of 2 m from the crystal at an angle $\Theta_D = 2\Theta_B = 22.5^\circ$. A square detector with a size of 10×10 μm is moved through the reflex center with 10 μm steps, which corresponds to the angular distribution measurement using an X-ray camera with the same pixel size. Curves 1 and 2 show the calculation results of the PXR and DTR angular distribution for a point-like unidirectional beam of particles ($\theta_e << \gamma^{-1}$). Curves 3 and 4 show that of the DTR for beam divergence of θ_e = 20 and 100 μrad, respectively. It is assumed that the angular distribution of the beam can be described by a two-dimensional Gaussian distribution, and a standard deviation corresponds to the typical divergence angle of the beam. The contribution of the diffracted bremsstrahlung and the spatial dimensions of the particle beam on

a crystal are not included. For simplicity, it is assumed that the values of the beam divergence in both planes are the same. With $\Theta_{ph} >> \theta_e$, the PXR angular distribution for the remaining θ_e is virtually identical and is therefore not presented.

Fig. 2 shows that the PXR contribution is concentrated in the observation angles $\theta_y > 0.5$ mrad and the maximum yield does not exceed $5 \cdot 10^{-13}$ photons/electron. At lesser angles, the PXR yield is less than 10^{-14} photon/electron. The DTR contribution is concentrated in the reflex center and amounts to more than the maximum PXR at 5 orders. Even for a beam divergence of 100 μrad, the DTR yield is 3 orders greater than the PXR yield. The intensity of higher PXR orders concentrated closer to the reflex center is substantially lower than the first order. In addition, the detection efficiencies of X-ray detectors are significantly decreased with increasing photon energy. The PXR contribution in the reflex center is thus negligibly small from analysis of the electron beam divergence and may be ignored. For selected conditions where the characteristic radiation angle $\gamma^{-1} \sim 2.5$ μrad is less than the detector angular capture $\upsilon_c = 5$ μrad, the dip in the center of the DTR angular distribution is absent, and its width (see curve 2 in Fig. 2) is not more than 3-4 steps of the detector. For this reason, the difference between the angular distributions for $\theta_e << \gamma^{-1}$ and $\theta_e = 20$ μrad is not very noticeable. The dependence obtained by processing the calculated standard deviations of the distributions σ_{calc} for the beam divergence θ_e is shown in the Fig. 3.

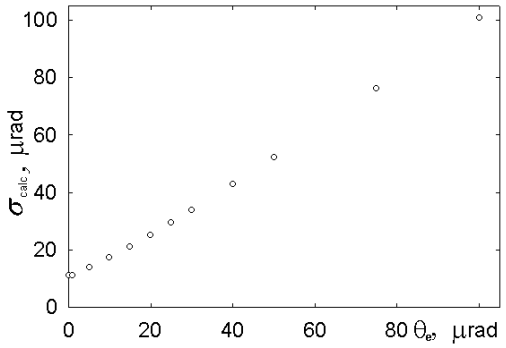

Fig. 3. Dependence of σ_{calc} on the beam divergence θ_e

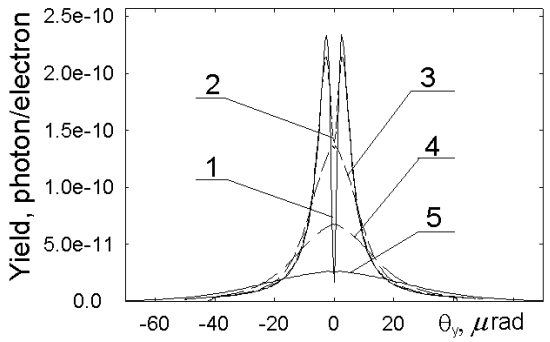

Fig. 4. Vertical distribution of the X-ray yield for an electron energy of 200 GeV and the first order reflection: 1 – DTR for $\theta_e << \gamma^{-1}$; 2 – DTR for θ_e =1 μrad; 3 – DTR for θ_e =5 μrad; 4 – DTR for θ_e =10 μrad; 5 – DTR for θ_e =20 μrad

For small values of beam divergence (θ_e<10 μrad), σ_{calc} is almost two times more than θ_e, and the values then begin to converge. σ_{calc} and θ_e practically coincide only when the condition $\theta_e >> \gamma^{-1}$ is satisfied.

To explain the dependence of σ_{calc} on the value of θ_e, calculations of the DTR angular distributions for a crystal to detector distance of 20 m, which corresponds to the angle of collimation $\vartheta_c \approx 0.5$ μrad ($<\gamma^{-1}) \approx$ 2.5 μrad were performed. The results of the calculations for electron beam divergence $\theta_e = 0.2$ ($<<\gamma^{-1}$), 1, 5, 10, and 20 μrad are shown in Fig. 4, respectively, where the PXR contribution was not taken into account.

Under these conditions, the DTR angular distribution appears as expected. There is a dip in the emission intensity for the strictly Bragg direction. A proportional broadening of the angular distribution for the detected radiation is observed as θ_e increases. The broadening is determined by a convolution of the angular distribution of the TR and that of the electron beam incident on the crystal, and since the angular distribution of the TR has a relatively long "tail", the angular distribution of the detected radiation begins to coincide with the form of that for the electron beam only when the condition $\theta_e >> \gamma^{-1}$ is satisfied.

The divergence of the beam and the transverse dimensions of the ILC in the horizontal and vertical planes are substantially different. Typical values for the divergence are $\theta_x \sim 50$ μrad and $\theta_y \sim 20$ μrad in the horizontal and vertical planes, respectively [1]. Accounting for this difference will lead to some reduction in the maximum intensity of the DTR angular distribution. However, if the condition $\theta_e >> \gamma^{-1}$ is satisfied, as with identical divergences in both planes, then the angular distribution of the detected radiation almost completely reproduces that of the particle beam incident on the crystal. If this condition is not satisfied, the desired value of θ_e can be obtained from the dispersion of the measured angular distribution and dependence shown in Fig. 3, or its analogue for the two-dimensional Gaussian distribution. Thus, by measuring the DTR angular distribution, information on the electron beam divergence in both planes can be obtained, and based on the measured or calculated emittance value, the beam size at the point of the measurement can be estimated.

The main barrier to the use of DTR in thin crystals to estimate electron beam divergence and spatial sizes is the destruction of the crystal structure under the influence of the intense electron beam during the measurement process. For example, in Ref. [29] (and references therein), the degradation of coherent effects for a 0.5 mm thick diamond crystal was observed at an electron energy of 16 GeV and a beam density of approximately 10^{19} electrons per cm^2. For the ILC with a spatial beam size of 100×5 nm, the beam density for one spill ($N_e \approx 2.6 \cdot 10^{13}$ electrons per spill) will be greater than the critical density for a 0.5 mm thick diamond crystal by several orders.

A possible solution to the crystal destruction problem may be the use of surface PXR (see Ref. [30] and references therein). This effect is related with the excitation of electrons in crystal atoms by the electromagnetic field of a charged particle moving near the crystal surface and its subsequent irradiation. To realize this phenomenon, it is necessary that the distance between the particle and the crystal edge is approximately $\gamma\lambda$ or less, where λ is the wavelength of the emission measured. The intensity of the radiation is close to the PXR inten-

sity with a correction factor of approximately $exp(-r/\gamma\lambda)$, where r is the distance between the particle trajectory and the crystal edge.

Surface PXR is similar to the Smith-Purcell effect [31], which is already used for electron beam parameter diagnostics in accelerator physics [5]. In both cases, the interference of electron radiation from atoms under the field influence of a charged moving particle is measured. However, the X-ray radiation wavelength for the experimental observation of this emission mechanism is small and has thus not been discussed yet. For the ILC and CLIC conditions, $\gamma\lambda$ becomes sub-millimeter; therefore, this type of radiation can be experimentally observed and used for electron beam parameter diagnostics.

However, here we have the same problem as with conventional PXR in crystals. The characteristic angular size of the PXR photon beam is far larger than the beam divergence measured. Because of practically whole analogy between surface and usual PXR we may wait existence of surface diffracted transition radiation with parameters closed to ordinary DTR. If this type of emission really exists then we may hope on its usage for measurement of high energy electrons beam parameters.

SUMMARY AND CONCLUSIONS

The results of the study may be briefly stated as follows:

1) The space resolution of any devices for X-ray beam spatial distribution measurements is limited by the size of the CCD pixel or the root-mean-squared path of the secondary electrons in the detector. The sizes of the planned electron-positron linear collider beams in both directions are far less than the typical size of a CCD pixel or other devices used for X-ray spatial distribution measurements. Therefore, PXR spatial distribution measurements cannot provide information regarding the sizes of such beams.

2) These data may be obtained from information on electron beam emittance in both planes and divergence, which may be obtained from measurements of an electron beam angular distribution. The beam emittance may be obtained from calculations or measurements at the earlier stages of acceleration using traditional methods with optical devices.

3) A typical value for the PXR characteristic angle is far greater than the ILC and CLIC beam divergences. Therefore, the influence of beam divergence on the PXR angular distribution is negligibly small. This type of fast electron emission in a crystal cannot facilitate beam divergence measurements.

4) For a particles energy approximately some hundreds of GeV, the DTR intensity in a narrow cone is far larger than the PXR intensity. The DTR angular distribution is compared with the electron beam angular distribution and may be used for measurement of the electron beam divergence.

5) In contrast to the Shintake monitor, the devices used in the proposed method are less expensive and may be installed in any part of the accelerator to control the electron beam parameters in the acceleration process.

6) The main barrier that can prevent the use of DTR in thin crystals for the estimation of electron beam divergence and spatial sizes is destruction of the crystal structure under the influence of a high intensity beam. For the ILC and CLIC conditions, crystal structure degradation can be expected after one spill of the accelerator. However, the proposed method may prove useful when the beam current is low, such as at the commissioning stage of the accelerator.

7) A possible solution to the crystal destruction problem may be the use of surface PXR. However, the same problem as with ordinary PXR in crystals can be expected. The characteristic angular size of the PXR photon beam is far larger than the measured beam divergence.

This work was supported by a grant from the Russian Science Foundation (Project N 15-12-10019).

REFERENCES

1. ILC Technical Design Report, 2013.
2. A Multi-TeV Linear Collider Based on CLIC Technology: CLIC Conceptual Design Report, 2012.
3. R.B. Fiorito. Recent Advances in Beam Diagnostic Techniques // *Proc. of PAC09*. 2009, p. 741.
4. J. Urakawa et al. Feasibility of optical diffraction radiation for a non-invasive low-emittance beam diagnostics // *NIM*. 2001, v. *A*472, p. 309.
5. G. Kube, H. Backe, W. Lauth, H. Schope. Smith-Purcell radiation in View of Particle Beam Diagnostics // *Proc. of DIPAC2003*. 2003, p. 40.
6. H. Loos et al. Observation of Coherent Optical Transition Radiation in the LCLS Linac // *Proc. of FEL08*. 2008, p. 485.
7. T. Shintake. Proposal of a nanometer beam size monitor for e+e− linear colliders // *NIM*. 1992, v. A311, p. 453.
8. J. Yan et al. Measurement of nanometer electron beam sizes with laser interference using Shintake Monitor // *NIM*. 2014, v. A740, p. 131.
9. A. Gogolev, A. Potylitsyn, G. Kube. A possibility of transverse beam size diagnostics using parametric X-ray radiation // *J. Phys. Conf. Ser.* 2012, v. 357, 012018.
10. Y. Takabayashi. Parametric X-ray radiation as a beam size monitor // *Phys. Lett. A*. 2012, v. 376, p. 2408.
11. G.M. Garibyan, C. Yang. Quantum Microscopic Theory of Radiation by a Charged Particle Moving Uniformly in a Crystal // *Sov. Phys. JETP*. 1972, v. 34, p. 495.
12. V.G. Baryshevsky, I.D. Feranchuk. Transition radiation of γ-rays in a crystal // *Sov. Phys. JETP*. 1972, v. 34, p. 502.
13. E.A. Bogomazova et al. Diffraction of real and virtual photons in a pyrolytic graphite crystal as source of intensive quasimonochromatic X-ray beam // *NIM*. 2003, v. B201, p. 276.
14. V.P. Lapko, N.N. Nanosov. On the parametric X-rays by a relativistic charged particle travelling through a crystal // *Sov. Phys. Tech. Phys.* 1990, v. 35(5), p. 633.
15. N.N. Nasonov. Collective effects in the polarization bremsstrahlung of relativistic electrons in condensed media // *NIM*. 1998, v. B145, p. 19.
16. H. Nitta. Theoretical notes on parametric X-ray radiation // *NIM*. 1996, v. B115, p. 401.

17. K.H. Brenzinger et al. Investigation of the production mechanism of parametric X-ray radiation // *Z. Phys.* 1997, v. *A*358, p. 107.
18. A.N. Baldin, I.E. Vnukov, E.A. Karataeva, B.N. Kalinin. O vklade difrakcii realnyx fotonov v nablyudaemye spektry parametricheskogo rentgenovskogo izlucheniya elektronov v sovershennyx kristallax // *Poverxnost.* 2006, № 4, s. 72-85 (in Russian).
19. K.H. Brenzinger et al. How narrow is the line width of parametric X-ray radiation // *Phys. Rev. Lett.* 1997, v. 79, p. 2462.
20. *High-Resolution X-Ray Camera*: http://www.proxivision.de/datasheets/X-Ray-Camera-HR25-x-ray-PR-0055E-03.pdf.
21. G. Kube, C. Behrens, A.S. Gogolev, Yu.P. Popov, A.P. Potylitsyn, W. Lauth, S. Weisse. Investigation of the applicability of parametric x-ray radiation for transverse beam profile diagnostics // *Proc. of IPAC2013*, 2013, p. 491.
22. A.L. Meadowcroft, C.D. Bentley, E.N. Stott. Evaluation of the sensitivity and fading characteristics of an image plate system for x-ray diagnostics // *Rev. Sci. Instrum.* 2008, v. 79, p. 113102.
23. Y. Takabayashi, K. Sumitani. New method for measuring beam profiles using a parametric X-ray pinhole camera // *Phys. Lett. A.* 2013, v. 377, p. 2577.
24. S.A. Laktionova, O.O. Pligina, M.A. Sidnin, I.E. Vnukov. Influence of real photons diffraction contribution on parametric X-ray observed characteristics // *J. Phys. Conf. Ser.* 2014, v. 517, 012020.
25. Yu.A. Goponov, S.A. Laktionova, O.O. Pligina, M.A. Sidnin, I.E. Vnukov. Influence of real photon diffraction on parametric X-ray radiation angular distribution in thin perfect crystals // *NIM.* 2015, v. B355, p. 150.
26. H. Nitta. Kinematical theory of parametric X-ray radiation // *Phys. Lett. A.* 1991, v. 158, p. 270.
27. В.И. Беспалов. Взаимодействие ионизирующих излучений с веществом. Томск, ТПУ. 2008, 396 с. V.I. Bespalov. *Vzaimodejstvie ioniziruyushhix izluchenij s veshhestvom.* Tomsk: TPU, 2008, 396 s.
28. I.D. Feranchuk, A.V. Ivashin. Parametric X-Ray: From the theoretical prediction to the first observation and applications // *J. Phys.* (Paris). 1985, v. 46, p. 1981.
29. R. Schwitters. *The SLAC Coherent Bremsstrahlung Facility*: SLAC-TN-70-32, 1970.
30. A.I. Benediktovitch, I.D. Feranchuk. Laser induced x-ray radiation under the grazing incidence geometry // *J. Phys. Conf. Ser.* 2010, v. 236, 012015.
31. S.J. Smith, E.M. Purcell. Visible Light from Localized Surface Charges Moving across a Grating // *Phys. Rev.* 1953, v. 92, p. 1069.

Article received 28.09.2015

ОЦЕНКА ПОПЕРЕЧНЫХ РАЗМЕРОВ ПУЧКА УЛЬТРАРЕЛЯТИВИСТСКИХ ЭЛЕКТРОНОВ ПО ИХ ИЗЛУЧЕНИЮ В ТОНКИХ КРИСТАЛЛАХ

Ю.А. Гопонов, М.А. Сиднин, K. Sumitani, Y. Takabayashi, И.Е. Внуков

Предлагается использовать излучение ультрарелятивистских электронов (позитронов) в тонких кристаллах для оценки размеров пучков проектируемых электрон-позитронных коллайдеров. Существующие позиционно-чувствительные детекторы рентгеновского диапазона и средний пробег вторичных электронов в детекторе ограничивают минимальное значение измеряемого размера пучка величиной порядка 10 мкм, что гораздо больше планируемых размеров пучков коллайдера. Предлагается оценивать расходимость пучка по угловым распределениям дифрагированного переходного излучения. Поперечные размеры могут быть получены из рассчитанного или измеренного значений эмиттанса пучка, определяемого на ранних стадиях ускорения с использованием оптических методов. Обсуждается проблема разрушения кристалла под действием электронного пучка. Предлагается для измерения параметров электронных пучков использовать поверхностное параметрическое рентгеновское излучение, где проблема разрушения кристалла полностью отсутствует.

ОЦІНКА ПОПЕРЕЧНИХ РОЗМІРІВ ПУЧКА УЛЬТРАРЕЛЯТИВІСТСЬКИХ ЕЛЕКТРОНІВ ЗА ЇХ ВИПРОМІНЮВАННЯМ У ТОНКИХ КРИСТАЛАХ

Ю.А. Гопонов, М.А. Сіднін, K. Sumitani, Y. Takabayashi, І.Є. Внуков

Пропонується використовувати випромінювання ультрарелятивістських електронів (позитронів) у тонких кристалах для оцінки розмірів пучків електрон-позитронних колайдерів, що проектуються. Існуючі позиційно-чутливі детектори рентгенівського діапазону і середній пробіг вторинних електронів у детекторі обмежують мінімальне значення вимірюваного розміру пучка величиною близько 10 мкм, що набагато більше планованих розмірів пучків колайдера. Пропонується оцінювати розбіжність пучка за кутовим розподілам дифрагованого перехідного випромінювання. Поперечні розміри можуть бути отримані з розрахованого або виміряного значень емітанса пучка, який визначається на ранніх стадіях прискорення з використанням оптичних методів. Обговорюється проблема руйнування кристала під дією електронного пучка. Пропонується для вимірювання параметрів електронних пучків використовувати поверхневе параметричне рентгенівське випромінювання, де проблема руйнування кристала повністю відсутня.